[3] I. M. De Rosa, F. Sarasini, M. S. Sarto, and A. Tamburrano, "EMC impact of advanced carbon fiber/carbon nanotube reinforced composites for next-generation aerospace applications," *IEEE Trans. Electromagn. Compat.*, vol. 50, no. 3, pp. 556–563, Aug. 2008.
[4] M. S. Sarto, A. G. D'Aloia, A. Tamburrano, and G. De Bellis, "Synthesis, modeling, and experimental characterization of graphite nanoplatelet-based composites for EMC applications," *IEEE Trans. Electromagn. Compat.*, vol. 54, no. 1, pp. 17–27, Feb. 2012.
[5] A. G. D'Aloia, F. Marra, A. Tamburrano, G. De Bellis, and M. S. Sarto, "Electromagnetic absorbing properties of graphene-polymer composite shields," *Carbon*, vol. 73, pp. 175–184, Jul. 2014.
[6] D. U. Sim, J. H. Kwon, Y. J. Chong, and S. O. Park, "Design of electromagnetic wave absorber using periodic structure and method to broaden its bandwidth based on equivalent circuit-based analysis," *IET Microw. Antennas Propag.*, vol. 9, no. 2, pp. 142–150, Feb. 2015.
[7] Y. Han, W. Che, C. Christopoulos, and Y. Chang, "Investigation of thin and broadband capacitive surface-based absorber by the impedance analysis method," *IEEE Trans. Electromagn. Compat.*, vol. 57, no. 1, pp. 22–26, Feb. 2015.
[8] R. X. Gao, W. J. R. Hoefer, and E. P. Li, "Quality synthesis based robust optimization for electromagnetic wave absorbers using Taguchi's tolerance design method," *IEEE Trans. Antennas Propag.*, vol. 62, no. 4, pp. 2102–2108, Apr. 2014.
[9] N. Zabri, R. Cahill, and A. Schuchinsky, "Polarisation independent resistively loaded frequency selective surface absorber with optimum oblique incidence performance," *IET Microw. Antennas Propag.*, vol. 8, no. 14, pp. 1198–1203, Nov. 2014.
[10] M. Mirsaneh, D. Furman, J. V. Ryan, M. T. Lanagan, and C. G. Pantano, "Frequency dependent electrical measurements of amorphous GeSbSe chalcogenide thin films," *Appl. Phys. Lett.*, vol. 96, pp. 1–3, Mar. 2010, Art. no. 112907.
[11] P. V. Wright, B. Chambers, A. Barnes, K. Lees, and A. Despotakis, "Progress in smart microwave materials and structures," *Smart Mater. Struct.*, vol. 9, pp. 273–279, Feb. 2000.
[12] O. G. Vendik, E. K. Hollmann, A. B. Kozyrev, and A. M. Prudan, "Ferroelectric tuning of planar and bulk microwave devices," *J. Supercond.*, vol. 12, no. 2, pp. 325–338, Apr. 1999.
[13] D. M. Pozar and V. Sanchez, "Tuning of a microstrip antenna on a ferrite substrate," *Electron. Lett.*, vol. 24, no. 12, pp. 729–731, Jun. 1988.
[14] K. S. Novoselov, V. I. Fal, L. Colombo, P. R. Gellert, M. G. Schwab, and K. Kim, "A roadmap for graphene," *Nature*, vol. 490, pp. 192–200, Oct. 2012.
[15] W. Zuojia *et al.*, "A circuit method to integrate metamaterial and graphene in absorber design," *Opt. Commun.*, vol. 329, pp. 76–80, Oct. 2014.
[16] B. Z. Xu, C. Q. Gu, Z. Li, L. L. Liu, and Z. Y. Niu, "Circuit model for graphene-based absorber at low-terahertz frequencies," *J. Phys. D, Appl. Phys.*, vol. 47, pp. 1–6, May 2014, Art. no. 255103.
[17] M. W. Woo, M. S. Kim, H. W. Kim, and J. H. Jang, "Graphene based Salisbury for terahertz absorber," *Appl. Phys. Lett.*, vol. 104, pp. 1–4, Feb. 2014, Art. no. 081106.
[18] S. He and T. Chen, "Broadband THz absorbers with graphene-based anisotropic metamaterial films," *IEEE Trans. Terahertz Sci. Technol.*, vol. 3, no. 6, pp. 757–763, Nov. 2013.
[19] O. Balci, E. O. Polat, N. Kakenov, and C. Kocabas, "Graphene-enabled electrically switchable radar-absorbing surfaces," *Nat. Commun.*, vol. 6, pp. 1–6, Mar. 2015, Art. no. 6628.
[20] Y. Zhang, Y. Feng, B. Zhu, J. Zhao, and T. Jiang, "Graphene based tunable metamaterial absorber and polarization modulation in terahertz frequency," *Opt. Express*, vol. 22, no. 19, pp. 22743–22752, Sep. 2014.
[21] A. Mohamed, K. Othman, G. Caner, and F. Capolino, "Graphene-based tunable hyperbolic metamaterials and enhanced near-field absorption," *Opt. Express*, vol. 21, no. 6, pp. 7614–7632, Mar. 2013.
[22] X. Huang, Z. Hu, and P. Liu, "Graphene based tunable fractal Hilbert curve array broadband radar absorbing for radar cross section reduction," *AIP Adv.*, vol. 4, pp. 1–12, Nov. 2014, Art. no. 117103.
[23] A. G. D'Aloia, M. D'Amore, and M. S. Sarto, "Terahertz shielding effectiveness of graphene-based multilayer s controlled by electric field bias in a reverberating environment," *IEEE Trans. Terahertz Sci. Technol.*, vol. 5, no. 4, pp. 628–636, Jul. 2015.
[24] M. Jablan, H. Buljan, and M. Soljačić, "Plasmonics in Graphene at Infrared Frequencies," *Phys. Rev. B*, vol. 80, no. 24, pp. 1–7, Dec. 2009.
[25] G. Hanson, "Dyadic Green's functions for anisotropic non-local model of biased graphene," *IEEE Trans. Antennas Propag.*, vol. 56, no. 3, pp. 747–757, Mar. 2008.
[26] Y. W. Tan *et al.*, "Measurement of scattering rate and minimum conductivity in graphene," *Phys. Rev. Lett.*, vol. 99, pp. 1–4, Dec. 2007, Art. no. 246803.
[27] K. S. Novoselov *et al.*, "Electric field effect in atomically thin carbon films," *Science*, vol. 306, pp. 666–669, Oct. 2004.
[28] J. H. Choi, Y. Mao, and J. P. Chang, "Development of hafnium based high-k materials—A review," *Mater. Sci. Eng. R Rep.*, vol. 72, no. 6, pp. 97–136, Jul. 2011.
[29] L. Qi, L. Petersson, and T. Liu, "Review of recent activities on dielectric films for capacitor applications," *J. Int. Counc. Electr. Eng.*, vol. 4, no. 1, pp. 1–6, Sep. 2014.
[30] L. A. Ponomarenko *et al.*, "Effect of a high-k environment on charge carrier mobility in graphene," *Phys. Rev. Lett.*, vol. 102, no. 20, pp. 1–4, May 2009.

Compact Microstrip Patch Array Antenna With Parasitically Coupled Feed

Dong-Fang Guan, Ying-Song Zhang, Zu-Ping Qian, Yujian Li, Wenquan Cao, and Feng Yuan

***Abstract*—A 3×3 parasitically coupled microstrip patch array antenna is proposed in this communication. The array consists of nine microstrip patches. The center patch fed by a probe works as a driven element while the other eight surrounding patches are parasitic elements. Four microstrip lines located between elements are employed as feed network to distribute coupled energy in both the E- and H-planes of the array. Thus, the 3×3 elements can be arranged on a single-layered substrate and excited simultaneously. The antenna has a simplified feed structure and a compact size. Meanwhile, the experimental results show that the proposed antenna has a broad bandwidth of 15.4% from 18 to 21 GHz and a maximum gain of 14.8 dBi.**

***Index Terms*—Antenna, compact structure, microstrip patch, parasitic array.**

I. Introduction

With the development of modern wireless communication systems, planar array antennas have been used for microwave and millimeter-wave applications such as satellite communications, remote sensing networks, and radar systems. Several types of planar array antennas have been reported in literature. Most traditional designs are microstrip patch antennas because of their low profile, compact size, low cost, and ease of integration with planar circuits [1].

Manuscript received July 10, 2015; revised January 10, 2016; accepted March 20, 2016. Date of publication March 25, 2016; date of current version May 30, 2016. This work was supported in part by the National Science Foundation of China under Grant 61271103 and in part by the Open Project of State Key Laboratory of Millimeter Waves, Southeast University China under Grant K201515.

D.-F. Guan and Y.-S. Zhang are with the College of Communications Engineering, PLA University of Science and Technology, Nanjing 210007, China, and also with the State Key Laboratory of Millimeter Waves, Southeast University, Nanjing 210007, China (e-mail: gdfguandongfang@163.com)

Z.-P. Qian, W. Q. Cao, and F. Yuan are with the College of Communications Engineering, PLA University of Science and Technology, Nanjing 210007, China.

Y. J. Li is with the Institute of Light Wave Technology, Beijing Jiaotong University, Beijing 100044, China.

Color versions of one or more of the figures in this communication are available online at http://ieeexplore.ieee.org.

Digital Object Identifier 10.1109/TAP.2016.2547019

0018-926X © 2016 IEEE. Personal use is permitted, but republication/redistribution requires IEEE permission.
See http://www.ieee.org/publications_standards/publications/rights/index.html for more information.

Authorized licensed use limited to: K.L. University(F.K.A. Koneru Lakshmaiah College of Engineering). Downloaded on November 09,2024 at 15:52:20 UTC from IEEE Xplore. Restrictions apply

Feed networks consisting of power dividers have been extensively used in designs of array antennas to split the input power into radiating elements with required amplitude and phase distributions. Generally, the microstrip array antennas can be divided into two groups: 1) series-fed arrays [2], [3] and 2) parallel-fed arrays [4], [5] according to the applied schemes of feed networks. These reported microstrip arrays have good radiation performance. However, the series-fed arrays suffer from a narrow impedance bandwidth, particularly with increase of the number of antenna elements. On the other hand, the parallel-fed networks usually have complex geometries which would occupy large space on substrate layers. Therefore, it is valuable to design a feed network with simple structure and wideband performance simultaneously.

Recently, microstrip array antennas with parasitically coupled feed networks have been reported [6]–[13]. In a parasitic array, only the driven element is directly excited while the other parasitic elements are excited through mutual coupling. Thus, the structure of the parasitic array is relatively simple and the loss of the array is reduced due to the short length of transmission lines in the feed network. Various techniques of parasitically coupled feed have been reported. The electrically steerable passive array radiators (ESPAR) were designed with parasitic elements to realize beam steering [6]–[8]. Multilayered parasitic microstrip arrays were reported in [9] and [10]. The parasitic elements arranged on the top layer of these designs were effectively excited by the driven element located on the bottom layer. In [11], parasitic elements were connected to the driven element by microstrip lines in the E-plane. Then the design was expanded to a 3×3 array in dual-layered structure. In [12] and [13], the coupling between patches in the H-plane was achieved through capacitive gaps between four radiating elements.

In this communication, a novel 3×3 parasitically coupled microstrip patch array is proposed. The center patch is a driven element and fed by a probe. The other eight surrounding patches work as parasitic elements. Four microstrip lines between them are employed to realize effective coupling. The antenna has a simple and compact structure, wide impedance bandwidth, and excellent radiation performance. The rest of the communication is organized as follows. Section II describes the configuration and design principle of the antenna. The experimental results and discussions are presented in Section III. Finally, a brief conclusion is given in Section IV.

II. Antenna Design

Fig. 1 shows two conventional coupling methods for parasitic patch arrays in single-layered geometry. To realize coupling in the E-plane, microstrip lines were introduced to connect adjacent patches [11]. On the other hand, the coupling in the H-plane was directly realized by tuning the spacing between adjacent elements [12]. In our design, two kinds of coupling methods are combined together. The coupling in the E- and H-planes can be achieved simultaneously in a single-layered structure. The antenna is designed by applying a Rogers-Duroid 5880 substrate with a relative dielectric constant of 2.2, and loss tangent of 0.0009. The thickness of the substrate h is 1.5 mm. The center frequency is designated at 20 GHz.

Fig. 2(a) and (b) gives the top and side views of the proposed array, respectively. As shown in Fig. 2(a), the array is composed of nine microstrip patches. The center patch is excited by a probe. The other eight surrounding patches are fed through coupling from the center element. Four microstrip lines are employed at four corners of the driven patch to fulfill the E-plane and H-plane coupling.

The design and optimization procedure is given as follows.

1) The length and width of the radiating patches (p_x and p_y), which mainly determine the operating frequency, are initially chosen as $\lambda_g/2$, where λ_g is the guided wavelength at 20 GHz.

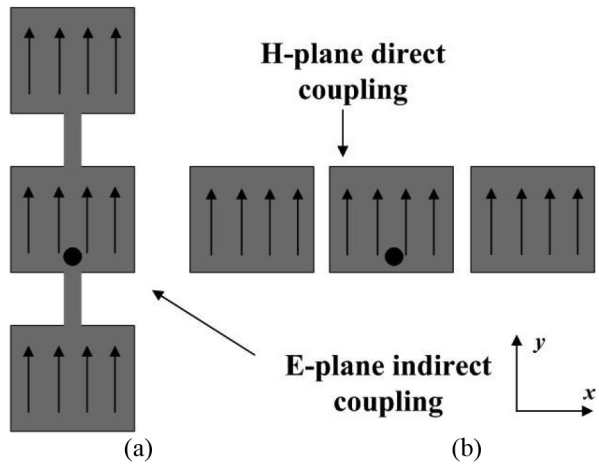

Fig. 1. Two coupled-fed methods. (a) Coupling in the E-plane. (b) Coupling in the H-plane.

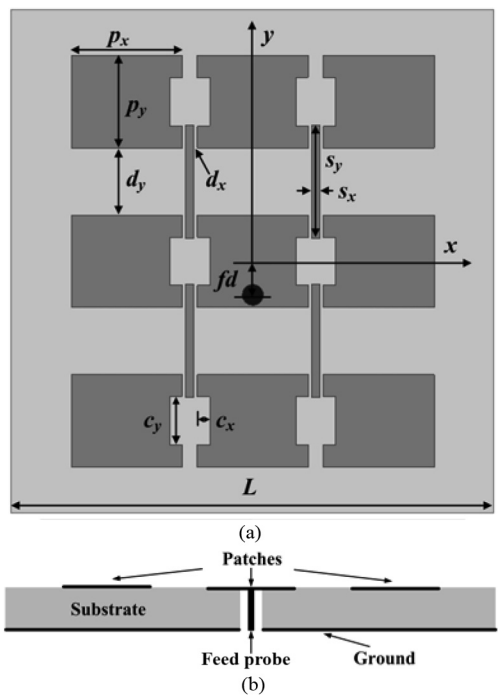

Fig. 2. Geometry of the proposed array antenna. (a) Top view. (b) Side view.

2) The size of the coupling microstrip lines (s_x and s_y) and the spacing between elements (d_x and d_y) are optimized such that all elements are excited in phase.

   It is found in the study that the capacitive gap d_x and the width of the microstrip line s_x are key parameters to control the H-plane coupling between patches. The length of microstrip line d_y is initially set as $\lambda_g/2$ to make an additional phase shift of 180°. Therefore, the three rows of patches in the E-plane can be fed in phase when the center element is excited.

3) The offset of the feeding probe f_d is used for impedance matching. Besides, additional slots with dimensions of c_x and c_y are cut at the two nonradiative edges of the patches to further improve the impedance matching of the array.

Fig. 3 shows the current direction and magnitude distributions on the top surface of the array at 20 GHz. It is seen that all the patches are

Authorized licensed use limited to: K.L. University(F.K.A. Koneru Lakshmaiah College of Engineering). Downloaded on November 09,2024 at 15:52:20 UTC from IEEE Xplore. Restrictions apply

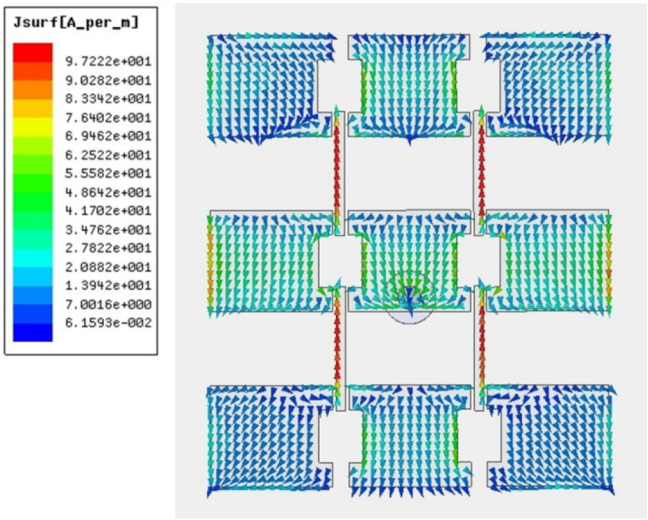

Fig. 3. Current distribution on the top surface of the array at 20 GHz.

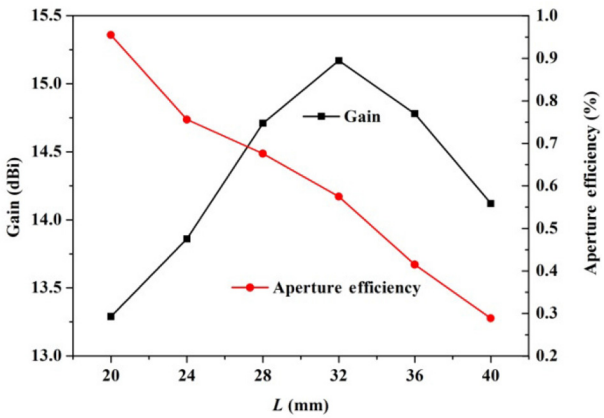

Fig. 4. Variation of gain and aperture efficiency of the array with different L at 20 GHz.

TABLE I
DIMENSION VALUES OF THE ARRAY (UNIT: MM)

p_x	p_y	d_x	d_y	s_x
5.3	4.4	0.15	3.2	0.4
s_y	c_x	c_y	fd	L
5.4	0.6	2.3	1.6	32

excited effectively, which demonstrates the effectiveness of the coupling in both planes. The current on the nine patches are in the same direction, which means that the patch array is fed in phase. Moreover, due to the center coupled feed method, the current magnitude distribution on the nine patches is slightly uneven. This would influence the aperture efficiency of the array, but the improvement of array gain can still be expected.

The length of the array ground plane is set as L, which would also influence the array gain. Fig. 4 shows the variation of gain and aperture efficiency at 20 GHz with different sizes of the ground plane. When $L = 20$, the size of the whole array is almost identical to the size of the nine radiating patches and the array gain is 13.29 dBi. With the increase in the ground plane, gain constantly increases and gets a maximal value of 15.17 dBi for $L = 32$ mm. After that, gain begins to decrease with the further increase in the ground plane size.

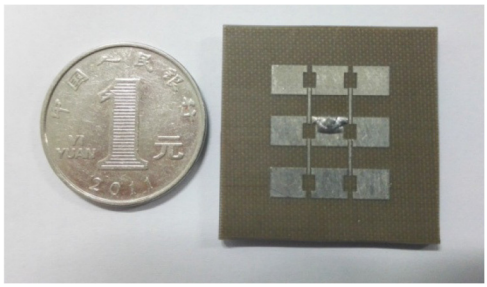

Fig. 5. Photograph of the fabricated prototype.

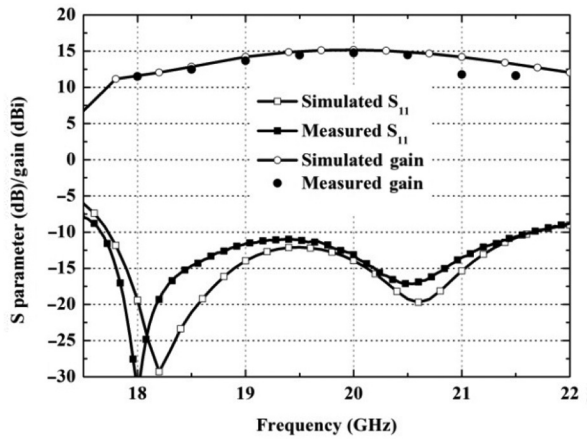

Fig. 6. Simulated and measured reflection coefficients and gains of the 3×3 array.

The aperture efficiency of the array is defined as $G/(4\pi A/\lambda_0^2)$, where G, A, and λ_0 are gain, physical size of the array, and the wavelength in free space at 20 GHz. As can be seen in Fig. 4, the aperture efficiency reduces from 95.5% to 28.9% with the size of the ground plane enlarged. The aperture efficiency is 57.5% for the maximum gain of 15.17 dBi.

III. EXPERIMENTAL RESULTS AND DISCUSSIONS

The dimension values of the array are optimized by the full wave software HFSS based on above studies. Final dimension values are listed in Table I. To validate the correctness of the design, a prototype is fabricated and tested as illustrated in Fig. 5.

The simulated and measured reflection coefficients and gains are depicted in Fig. 6. The measured impedance bandwidth of the antenna is 20.4% from 17.65 to 21.65 GHz. A slight shift in frequency can be seen compared to the simulated one, which is mainly caused by the fabrication tolerance. The gain and radiation pattern are measured in a chamber with a far-field measuring setup. The measured gain agrees well with the simulated one. The measured 3-dB gain bandwidth is from 18 to 21 GHz and the maximum value of gain is 14.8 dBi. The overlapped operating bandwidth between the impedance and 3-dB gain bandwidths of the array is 15.4%.

Fig. 7 shows the simulated and measured radiation patterns of the array at 19, 20, and 21 GHz, which are in good agreement. The 3-dB beamwidths in both the E- and H-planes are around 20°. The cross-polarization levels are less than -18 dB and the measured first sidelobe levels are less than -13 dB.

A detailed comparison between reported designs and this work is illustrated in Table II. It can be seen that the proposed 3×3 array antenna has a simple structure and a compact size compared with the

Authorized licensed use limited to: K.L. University(F.K.A. Koneru Lakshmaiah College of Engineering). Downloaded on November 09,2024 at 15:52:20 UTC from IEEE Xplore. Restrictions apply

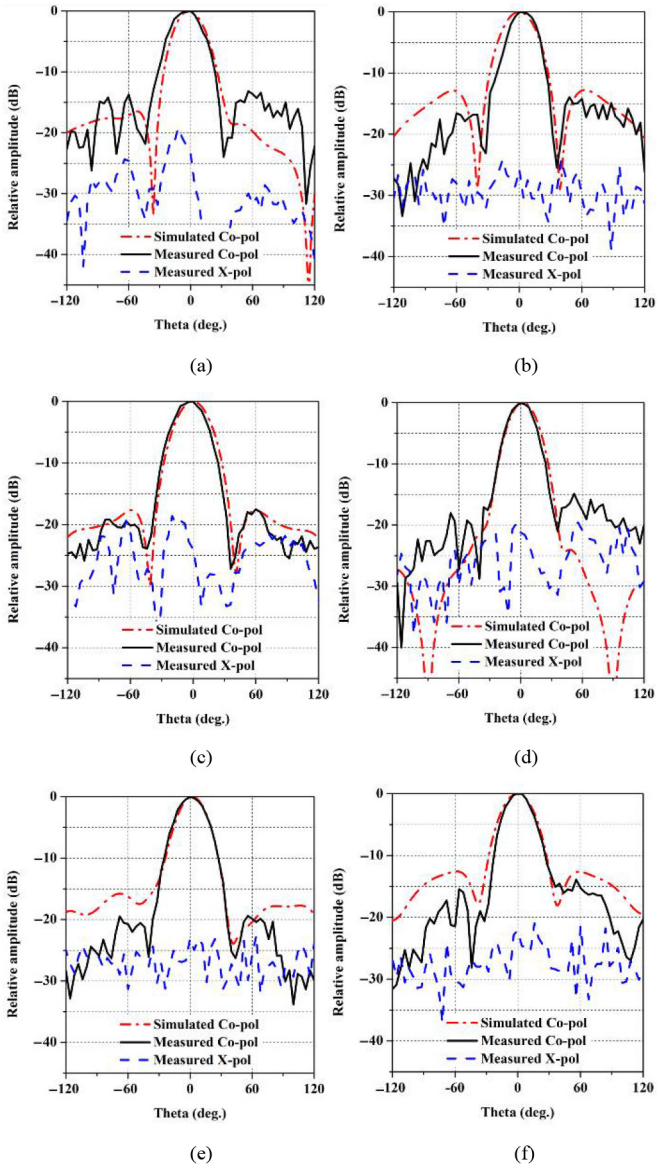

Fig. 7. Simulated and measured normalized radiation patterns in (a) E-plane at 19 GHz; (b) H-plane at 19 GHz; (c) E-plane at 20 GHz; (d) H-plane at 20 GHz;, (e) E-plane at 21 GHz; and (f) H-plane at 21 GHz.

TABLE II
THE COMPARISON BETWEEN DIFFERENT PARASITIC ARRAY ANTENNAS

	No. of layer	No. of element	Size (λ_0)	Bandwidth (%)	Gain (dBi)	Aperture efficiency (%)
[9]	4	9	2×2	5.5	11.1	25.6
[11]	2	9	2.25×2.25	/	16.5	70.2
[12]	1	4	1.36×0.97	8.6	11.6	87.2
our work	1	9	2.13×2.13	15.4	14.8	53

other three designs. More importantly, the bandwidth of this design is much wider than other reported works. Finally, the gain of the proposed array is also comparable to those parasitic array antennas in the literature.

IV. CONCLUSION

A novel 3 × 3 parasitically coupled microstrip patch array antenna is proposed in this communication. By employing four microstrip lines between adjacent patches, eight surrounding parasitic patches can be fed effectively by the center driven element. The antenna has a simple structure and a compact size. Meanwhile, wide bandwidth and high-gain performance are achieved as well.

REFERENCES

[1] D. M. Pozar, "Microstrip antennas," *Proc. IEEE*, vol. 80, no. 1, pp. 79–91, Jan. 1992.
[2] I-J. Chen, C.-S. Huang, and P. Hsu, "Circularly polarized patch antenna array fed by coplanar waveguide," *IEEE Trans. Antennas Propag.*, vol. 52, no. 6, pp. 1607–1609, Jun. 2004.
[3] T. Yuan, N. Yuan, and L.-W. Li, "A novel series-fed taper antenna array design," *IEEE Antennas Wireless Propag. Lett.*, vol. 7, pp. 362–365, Jul. 2008.
[4] M. M. Bilgic and K. Yegin, "Wideband offset slot-coupled patch antenna array for X/Ku-band multimode radars," *IEEE Antennas Wireless Propag. Lett.*, vol. 13, pp. 157–160, Jan. 2014.
[5] S. Ye, J. P. Geng, X. L. Liang, Y. Jay Guo, and R. H. Jin, "A compact dual-band orthogonal circularly polarized antenna array with disparate elements," *IEEE Trans. Antennas Propag.*, vol. 63, no. 4, pp. 1359–1364, Apr. 2015.
[6] H. Kawakami and T. Ohira, "Electrically steerable passive array radiator (ESPAR) antennas," *IEEE Antennas Propag. Mag.*, vol. 47, no. 2, pp. 43–50, Apr. 2005.
[7] Y. Yusuf and X. Gong, "A low-cost patch antenna phased array with analog beam steering using mutual coupling and reactive loading," *IEEE Antennas Wireless Propag. Lett.*, vol. 7, pp. 81–84, Apr. 2008.
[8] J. J. Luther, S. Ebadi, and X. Gong, "A microstrip patch electronically steerable parasitic array radiator (ESPAR) antenna with reactance-tuned coupling and maintained resonance," *IEEE Trans. Antennas Propag.*, vol. 60, no. 4, pp. 1803–1813, Apr. 2012.
[9] T. Seki, N. Honma, K. Nishikawa, and K. Tsunekawa, "Millimeterwave high-efficiency multilayer parasitic microstrip antenna array on Teflon substrate," *IEEE Trans. Microw. Theory Techn.*, vol. 53, no. 6, pp. 2101–2106, Jun. 2005.
[10] T. Seki, N. Honma, K. Nishikawa, and K. Tsunekawa, "A 60-GHz multilayer parasitic microstrip array antenna on LTCC substrate for system-on-package," *IEEE Microw. Wireless Compon. Lett.*, vol. 15, no. 5, pp. 339–341, May 2005
[11] S.-W. Qu, Sr., C. H. Chan, M.-Y. Xia, and Z. Nie, "High-efficiency periodic sparse microstrip array based on mutual coupling," *IEEE Trans. Antennas Propag.*, vol. 61, no. 4, pp. 1963–1970, Apr. 2013.
[12] S. H. Yeung, A. García-Lampérez, T. K. Sarkar, and M. Salazar-Palma, "Comparison in performance between a parasitically coupled and a direct coupled feed for a microstrip antenna array," *IEEE Trans. Antennas Propag.*, vol. 62, no. 5, pp. 2813–2818, May 2014.
[13] S. H. Yeung, A. García-Lampérez, T. K. Sarkar, and M. Salazar-Palma, "Thin and compact dual-band four-element broadside patch antenna arrays," *IEEE Antennas Wireless Propag. Lett.*, vol. 13, pp. 567–570, Apr. 2014.

uthorized licensed use limited to: K.L. University(F.K.A. Koneru Lakshmaiah College of Engineering). Downloaded on November 09,2024 at 15:52:20 UTC from IEEE Xplore. Restrictions apply